

Reflectivity Change in Nanoscale Modification of DLC Film with Femtosecond Laser Pulses

Godai MIYAJI*, Wataru KOBAYASHI* and Kenzo MIYAZAKI*

*Institute of Advanced Energy, Kyoto University, Gokasho, Uji, Kyoto 611-0011, Japan
E-mail: g-miyaji@iae.kyoto-u.ac.jp

We have measured the reflectivity of fs-laser irradiated diamond-like carbon (DLC) film, using the pump and probe technique, to understand interaction processes responsible for the bonding structure change and the nanostructure formation that were recently observed in the low-fluence ablation of DLC surface. The results have shown that the characteristic reflectivity change observed as a function of the superimposed laser shots is correlated with the selective change in the bonding structure from sp^3 to sp^2 to induce a swelling of the film surface, and that the nanostructure formation on the DLC surface is certainly preceded by the change in the bonding structure. The experimental results suggest that a local field created with the low fluence fs laser pulse plays an essential role to form the periodic nanostructure on the film surface.

Keywords: Femtosecond laser ablation, nanostructure formation, surface modification, diamond-like carbon, local field

1. Introduction

New fields of materials processing and machining have been developed with the excellent characteristics of intense femtosecond (fs) laser pulses that can deposit a high energy into a variety of materials in an ultrashort time through non-thermal processes [1,2]. Recently, it has been found in an attempt to use the fs laser pulses for nanostructuring of hard thin films such as TiN and diamond-like carbon (DLC), that the thin film surface can be structured periodically on a nanometer level when the fs laser pulses are irradiated at an energy fluence around the ablation threshold [3-5]. The size of periodic structure observed is 1/10 – 1/5 of the fs-laser wavelength, and the surface morphology can be controlled by the laser fluence, wavelength and polarization. A similar periodic surface structure, so-called ripples, is known to appear in the laser ablation of materials, which is understood as a phenomenon arising from the interference of an incident laser light with its scattered wave on the material surface [6,7], and the structure size is on the order of laser wavelength. However, the nanostructure reported so far is much smaller than the laser wavelength or the ripple size [3-5], implying that the nanostructure formation process is different from that for the ripple. Although the physical process for the nanostructure formation is not understood yet, much attention has been focused on this phenomenon, because it suggests a promising approach to nanometer-scale control and characterization of materials with fs laser pulses.

Moreover, the low-fluence fs laser pulses have been found to modify the DLC surface into a glassy carbon (GC) layer under almost the same condition as for the nanostructure formation [8,9]. This surface modification shows that the sp^3 bonds in DLC are selectively changed to sp^2 to form the GC layer, whereas DLC is composed of sp^3 and sp^2 bonds. In the previous experiment [9] we measured the reflectivity change on the DLC surface

irradiated with the fs laser pulses. Although the results have shown that the reflectivity is able to provide a good measure to monitor the interaction process on the surface, further study is required to understand the detail of the ultrafast interaction processes.

In this paper, we report the results of reflectivity measurements made with a pump-probe technique to understand the interaction process responsible for the structural change from DLC to GC and the nanostructure formation on the DLC surface. The characteristic changes in reflectivity observed demonstrate that the selective bonding structure change from sp^3 to sp^2 induces a swelling of the film surface, and this change in bonding structure certainly precedes the periodic nanostructure formation. Based on the results obtained, we propose that a localized field is created on a nanometer level and play an essential role to form the periodic nanostructure on the film surface.

2. Experimental

The DLC film [10] used as the target was deposited on Si substrates with a magnetron sputtering system. The film thickness is 1.6 μm , and Cr and composite W/C films are inserted as buffer layers between DLC and the Si substrate. The surface roughness (root-mean-square value) was measured to be ~ 15 nm with a scanning probe microscope (SPM), which was much smaller than that of DLC film deposited on a stainless steel plate in the previous experiments [3-5,8,9].

Figure 1 shows the experimental setup for reflectivity measurements using the pump and probe technique. We used a Ti:sapphire laser system that produced 100-fs, 800-nm pulses at a repetition rate of 10 Hz. The laser beam is linearly polarized with a well-defined lowest-order Gaussian profile of 5 mm diameter. The output is split into two beams with a half mirror (HM) to produce a pump and a probe pulse. The pump pulse is irradiated for ablation of the DLC surface, while the probe pulse is used

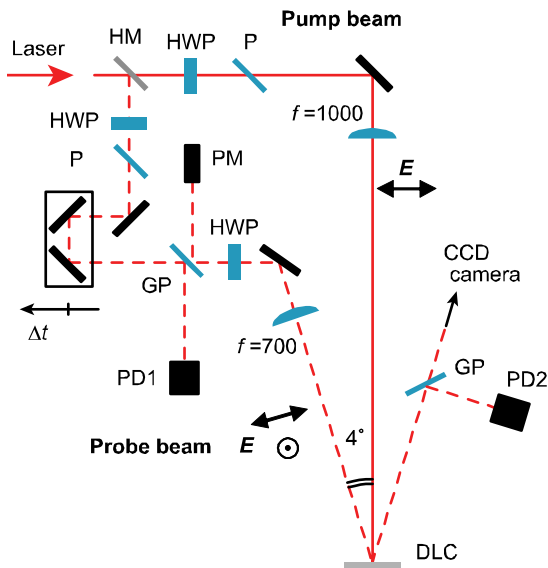


Fig. 1 Schematic diagram of the experimental arrangement for the reflectivity measurement using the pump-probe technique.

to measure the reflectivity R of the DLC. The pump pulse is focused in air at normal incidence onto the DLC with a lens of 1000-mm focal length. The focal spot was $230 \mu\text{m}$ in $1/e^2$ diameter, and the laser fluence F was varied in a range of $F = 0.06 - 0.2 \text{ J/cm}^2$ with a pair of half-wave plate (HWP) and polarizer (P). On the other hand, the probe pulse is focused at an incident angle of 4° with a 700-mm focal-length lens, of which focal spot size is $160 \mu\text{m}$ in $1/e^2$ diameter and completely overlapped to the center of the pump focal spot. The time delay Δt between the pump and probe pulses is changed in a range of $\Delta t = 0 - 70 \text{ ps}$. Observing the interference fringes on the target plane with a CCD camera, we controlled the temporal and spatial overlapping of the pump and probe pulses at $\Delta t = 0$. The probe pulse fluence is suppressed to 0.2 mJ/cm^2 , which is less than $1/300$ of the pump, so that the probe pulse never induces any structural change of the DLC film. The probe pulse polarization is rotated with a half-wave plate (HWP) placed in front of the focal lens when necessary.

Throughout the present experiment, the reflectivity R to be measured is defined by the ratio of the incident probe pulse energy to the pulse energy detected in the direction at the angle of reflection. The measurement of R is made by separating a small portion of the incident and reflected pulses with a glass plate (GP) and detecting it with a calibrated Si/PIN photodiode (PD1 and PD2). The detected pulse energy was recorded and stored for every laser shot on a digital storage oscilloscope. In the experiment, the laser pulses of $N = 1 - 1000$ shots were superimposed at different fluences.

The surface morphology was observed with the SPM, and the modification of bonding structure was analyzed with Raman spectroscopy using the 514.5-nm line of a focused argon ion laser beam, of which spot size was $10 \mu\text{m}$, corresponding to an excitation power density of 0.2 MW/cm^2 so as to avoid the damage on DLC films.

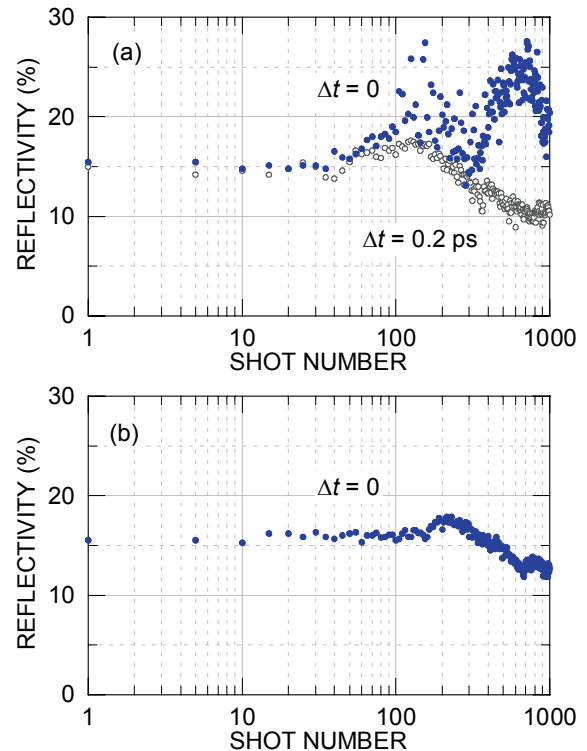


Fig. 2 Reflectivity measured as a function of N at (a) $\Delta t = 0$ (blue circles) and 0.2 ps (white circles) for parallel polarizations and at (b) $\Delta t = 0$ for perpendicular polarizations. The pump fluence is $F = 0.13 \text{ J/cm}^2$.

3. Results

Figure 2 shows typical examples of R measured as a function of N for $F = 0.13 \text{ J/cm}^2$, where the pump and probe polarizations are (a) parallel and (b) perpendicular. We note in Fig.2(a) that with an increase in N , the reflectivity R at $\Delta t = 0$ is peaked with $N \sim 160$ and ~ 700 . Such an enhancement of R has never been observed with the probe polarization perpendicular to the pump, as shown in Fig.2(b). Furthermore, even for the parallel polarization we did not observe the enhancement of R at $\Delta t \geq 0.2 \text{ ps}$, as seen in Fig.2(a). It should be noted that the characteristic change in R for the parallel polarization is observed with the weak probe pulse of which fluence is $\sim 1/700$ of the pump. These results suggest that the enhancement of R is induced through a coherent interaction between the probe pulse and the DLC surface excited with the pump pulse.

It is clear that the enhancement of R is induced by such an *incubation effect* that accumulates or stores a portion of the laser pulse energy in the target material, since the pump pulse fluence used in the reflectivity measurement is less than the single-pulse ablation threshold. To see the effect of the pump fluence we measured R at $F = 0.11 - 0.18 \text{ J/cm}^2$, keeping the probe pulse fluence at 0.2 mJ/cm^2 . The results are shown in Fig.3. For $F = 0.11 \text{ J/cm}^2$, the small enhancement of R is observed around $N \sim 800$. With an increase in F , the position of enhanced R is shifted to a region of smaller number of N , and two clear peaks are observed to appear around $N \sim 330$ and ~ 520 in Fig.3(b),

$N \sim 140$ and 460 in Fig.3(c), and $N \sim 25$ and ~ 50 in Fig.3(d). For $F = 0.18 \text{ J/cm}^2$, as seen in Fig.3(e), only a single peak is observed at $N \sim 10$. We have observed that at $N \sim 1000$ for $F = 0.14 \text{ J/cm}^2$, the DLC layer was completely removed from the central focal area of the film surface by the ablation, and the underlying layer was revealed. For $F = 0.17$ and 0.18 J/cm^2 , the complete removal of the DLC layer was observed to take place at $N \sim 100$ where the measurement was stopped. The results shown in Fig.3 clearly demonstrate that the enhancement of R observed as a function of N is certainly induced by the incubation effect depending on the pump fluence.

Keeping the above results in mind, we observed the DLC film surfaces with the SPM to study the correlation between the characteristic change in R and the surface morphology. Several DLC samples were irradiated with different numbers of N at a fixed fluence of $F = 0.14 \text{ J/cm}^2$, and the target surface was observed with the SPM. Figure 4 shows the SPM images of the DLC surface irradiated with (a) $N = 0$ (non-irradiated), (b) 130 and (c) 500, where those observed for the central areas of $30 \mu\text{m} \times 30 \mu\text{m}$ and $1 \mu\text{m} \times 1 \mu\text{m}$ are arranged up in the upper and middle lines, respectively. The non-irradiated surface shown in Fig.4(a) shows the surface roughness of $\sim 15 \text{ nm}$, as mentioned above. For the target irradiated with $N = 130$, where R is peaked as shown in Fig.3(c), we have observed that an interference pattern is formed in the central focal area of about $50 \mu\text{m}$ diameter, as seen in the upper of Fig.4(b). The spacing of interference fringe are measured to be $\Lambda \sim 11 \mu\text{m}$ with the averaged height of $\sim 100 \text{ nm}$, which corresponds to $\Lambda = \lambda/\sin\theta$ with the laser wavelength $\lambda = 800 \text{ nm}$ and the angle $\theta = 4^\circ$ between the probe and the pump beams. The fringe height was also measured by scanning the SPM over an area of $100 \mu\text{m} \times 100 \mu\text{m}$ including the focal point and the non-irradiated surface, and then it has been found that the interference fringe is formed by an increase in height of the DLC surface irradiated with the pump and probe pulses. Such swelling of the DLC surface has been observed so far in the fs laser ablation experiments [4,11,12]. We demonstrate later that this swelling is certainly due to the structural change from DLC to GC, being accompanied with the mass density change from $2.1 - 2.9 \text{ g/cm}^3$ for DLC [13] and to $1.3 - 1.55 \text{ g/cm}^3$ for GC [14].

As seen in the middle image of Fig.4(b), the surface morphology appears to be slightly changed by the swelling, compared with the surface image shown in Fig.4(a), but the ablation to form the periodic fine structure is never induced with this shot number of $N = 130$. With an increase in N to 300, the swelled surface is observed to become shallow due to ablation initiated at the crest. With $N \sim 500$, the nanostructure is formed as shown in Fig.4(c). As seen with the lower traces in Fig.4, the nanostructure observed at $N = 500$ has a depth of $\sim 100 \text{ nm}$, while the surface modulation or roughness is on the order of 10 nm before the initiation of ablation.

Based on these results, we may conclude that the enhancement of R shown in Figs.2 and 3 is predominantly due to the formation of the interference fringe that works as a holographic grating or a hologram. In this case, the pump pulse can partially be diffracted to the direction of

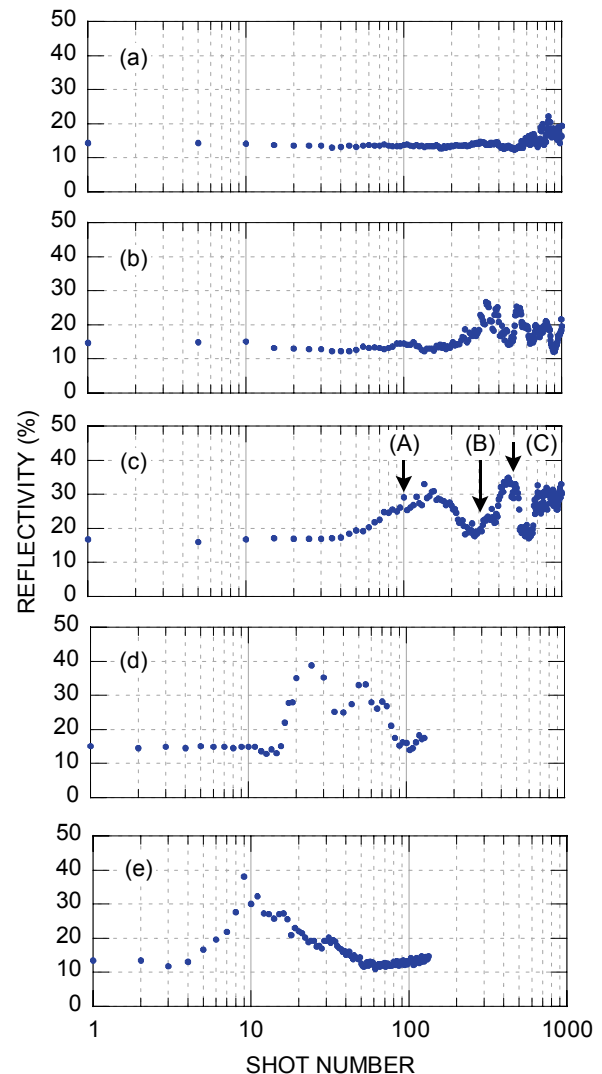


Fig. 3 Reflectivity measured with the probe pulses at $\Delta t = 0$ as a function of N for (a) $F = 0.11$, (b) 0.12 , (c) 0.14 , (d) 0.17 , and (e) 0.18 J/cm^2 . The pump and probe polarizations are parallel.

the reflected probe beam to increase R . Using a weak laser pulse we have confirmed that the normal incident beam is diffracted to the direction at an angle of 4° on the DLC surface having the interference fringe. The diffraction efficiency of the grating formed with $N = 130$ in Fig.4(b) was measured to be $\sim 0.5 \%$. It is easily estimated that this diffraction efficiency leads to an increase in the signal of R by about 20% , comparing the incident pump pulse energy with the reflected probe pulse energy. Taking into account the reflectivity of $R \sim 15 \%$ at the non-irradiated DLC surface, the reflectivity to be observed with $N \sim 130$ is $R \sim 35 \%$, being in good agreement with the observed one of $R \sim 33 \%$, as seen in Fig.3(c). With an increase in N , the grating groove with the spacing of $\sim 11 \mu\text{m}$ is observed to become shallow owing to the initiation of ablation, while the nanostructure start to be formed, as seen in Fig.4(c).

The holographic grating formed on the DLC surface is also able to produce a diffracted wave that propagates to

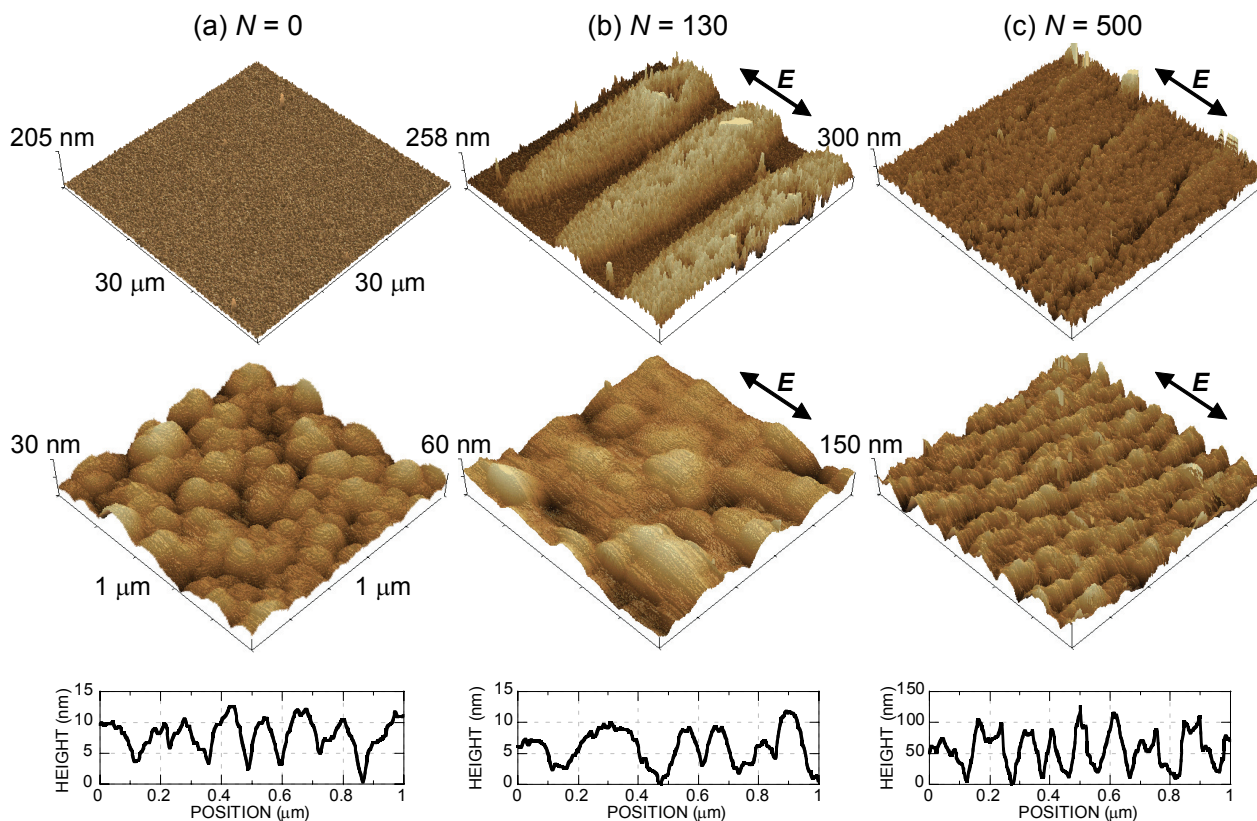


Fig. 4 SPM images of the DLC surfaces irradiated with (a) $N = 0$, (b) 130 and (c) 500 for $F = 0.14 \text{ J/cm}^2$ under the same conditions as in Fig.3(c). The upper and middle images are for the central areas of $30 \mu\text{m} \times 30 \mu\text{m}$ and $1 \mu\text{m} \times 1 \mu\text{m}$ on the focal spot, respectively. The lower images are the height profiles on the surface along the polarization direction denoted by the arrows.

the backward direction with respect to the incident probe pulse. In the present experiment, this negatively diffracted light would be regarded as the phase-conjugate wave [15]. We detected the backward signal with a photomultiplier (PM) in Fig.1. A typical example of the backward signal is shown in Fig.5, which has been observed simultaneously with R at $\Delta t = 0$ shown in Fig.2(a). We could never observe such backward signal with the probe polarization perpendicular to the pump. These results are consistent with the above conclusion that the enhanced signal for R in Figs.2 and 3 is due to the grating formation on the DLC surface.

The backward signal shown in Fig.5 represents two peaks at $N \sim 170$ and ~ 410 , which correspond to those observed at $\Delta t = 0$ in Fig.2(a). As discussed above, the first peak is induced in the region of N by the initial bonding change with no ablation. The second peak is much larger than the first. This is in contrast to the second peak seen in Fig.2(a), which should be a superposed signal consisting of the decreased probe signal, as for $\Delta t = 0.2 \text{ ps}$ in Fig.2(a), and the strongly diffracted pump signal. As shown in Fig.4 (also see the result shown Fig.6), the second peak in the backward signal appears in the region of N where the nanostructure is formed on the surface. This suggests that the nanostructure formation contributes to the increase in the diffraction efficiency due most likely to the improved surface smoothness on the laser wavelength scale

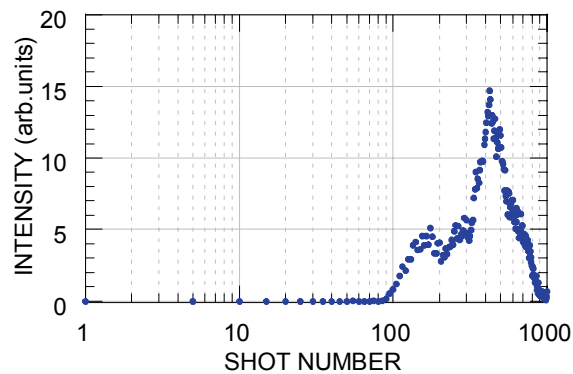


Fig. 5 Phase-conjugate signal measured as a function of N at $\Delta t = 0$ under the same conditions as in Fig.2(a).

or less. Such smoothness has been observed so far in the laser ablation of DLC surface [8]. On the other hand, the second signal peak in Fig.2(a) is shifted to a region of the larger number of N . Although the origin of this shift is not clear, the probe pulse reflection would be affected with the interference and/or scattering at the surface that dynamically changes with an increase in N .

To see the detailed correlation of R with the nanostructure formation on the surface, we measured the mean spacing l and depth d of the nanostructure as a function of N at $F = 0.14 \text{ J/cm}^2$ for $\Delta t = 0$, using the SPM, and the result is shown in Fig.6. The periodic nanostructures with $l = 80 - 110 \text{ nm}$ are observed in a range of $N = 300 - 900$. With $N \sim 1000$, the DLC layer was completely removed from the central focal area of the film surface. It should be noted in Fig.6 that the nanostructure starts to be observed at $N \sim 300$, where R decreases down to a minimum after the first peak. With an increase in R from the minimum, the structure depth increases to form the deepest groove in the region of the second peak of R around $N \sim 500$.

As discussed above, the swelling to form the grating on the DLC film should be due to the modification of the bonding structure in the DLC layer. To confirm this, we observed the Raman spectrum of the interference patterns swelled on the DLC surface. Figure 7 shows the results for the target irradiated with $N = 100$ (a), 300 (b) and 500 (c) at the pump fluence of $F = 0.14 \text{ J/cm}^2$, together with the spectrum of the non-irradiated DLC for comparison, where each spectrum corresponds to the different target marked as (A), (B) and (C) in Fig.3(c). The spectrum of the non-irradiated DLC shows a peak at the shift of $\sim 1530 \text{ cm}^{-1}$, as seen in Fig.7(d), whereas those (a), (b) and (c) represent the GC spectra including two peaks that are characterized by a large peak at 1355 cm^{-1} and a smaller one at 1590 cm^{-1} [8,9]. The Raman spectrum shown in Fig.7(a) demonstrates that the structural change from DLC to GC is induced already with $N \sim 100$ around the first enhancement of R in Fig.3(c), where the nanostructure is not formed yet, as seen in Fig.4(b). This indicates that the change in bonding structure from DLC to GC precedes the nanostructure formation. We note that, as shown in Fig.7(a), this structural change is induced with $N \sim 100$ around the first peak (A) of R in Fig.3(c), where neither ablation nor nanostructure formation is induced yet, as

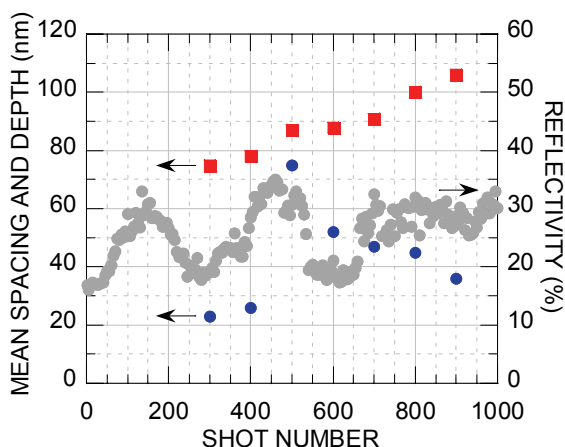


Fig.6 Mean spacing (red squares) and depth (blue circles) of periodic structures measured with the SPM as a function of N for the DLC irradiated under the same conditions as in Fig.3(c). Gray circles represent the change in R measured as a function of N .

shown in Fig.4(b). In Fig.7(b) the spectral peaks become smaller than in Fig.7(a). This suggests that the partial content of GC in the surface layer is decreased at $N \sim 300$ where R is almost minimized at (B) in Fig.3(c). The most distinct GC spectrum having the larger peak at 1355 cm^{-1} than at 1590 cm^{-1} is observed at $N \sim 500$, as shown in Fig.7(c), where the second peak (C) of R appears in Fig.3(c). These results show that the change in R on the DLC films is correlated with the change in bonding structure of the film surface.

4. Discussion

Based on the results obtained as a function of N , we discuss on the interaction process for the structural change of DLC surface. It should be noted that the present experiment was made at the laser fluence less than the single-pulse ablation threshold. With an increase in N , the fs laser pulses first induce the surface modification from DLC to GC. The structural change corresponds to the transition of the sp^3 bonds in DLC to the different stable structure of the sp^2 for GC. This selective transition should be induced owing to the sp^3 dissociation energy smaller than the sp^2 [9]. The pump pulse energy is partially stored in the thin film through the structural change, which is an incubation effect in the ablation process of the DLC film [9]. In the experiment using the pump and probe technique, the bonding change is clearly detected as the surface swelling to form the grating before the ablation. With a further increase in N , the swelled GC layer starts to be ablated from the surface to form the nanostructure, where the sp^2 bonds tend to preferentially be ionized with the fs laser pulses due to the lower ionization energy (or band gap) than that of the sp^3 . Thus, the change in the bonding structure from DLC to GC certainly precedes the ablation to form the nanostructure.

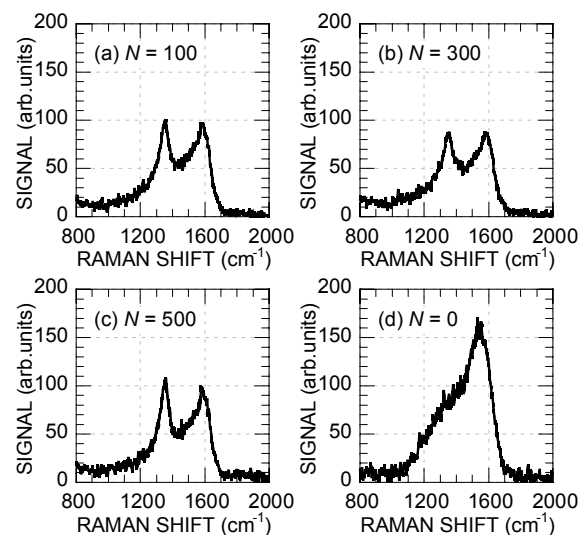


Fig.7 Raman spectra of DLC surfaces irradiated with (a) $N = 100$, (b) 300, and (c) 500 at $F = 0.14 \text{ J/cm}^2$ together with (d) the spectrum of non-irradiated DLC. The experimental conditions for (a), (b) and (c) are the same as those at (A), (B), and (C) in Fig.3(c).

The results shown in Fig.6 indicates that the measurable shallow nanostructure is formed with $N \sim 300$ at $F = 0.14 \text{ J/cm}^2$. This suggests that the nano-scale ablation to form the fine structure starts to locally be induced in a region of $N < 300$. In fact, as mentioned before, no ablation is observed with $N \sim 130$, where the reflectivity R is peaked due to the largest swelling to form the grating. It is reasonable to consider that the decrease in R for $N > \sim 130$ suggests that the nano-scale ablation would preferentially take place in the swelled surface. This is consistent to the fact that the ionization potential of the sp^2 bond is lower than that of the sp^3 [14] in the DLC, and free electrons would more efficiently be produced in the swelled surface of GC than in the original DLC layer to initiate the local ablation. This ablation should lower the swelled volume and resulting diffraction efficiency or R . The partial removal of the GC volume is suggested by the spectrum shown in Fig.7(b), which represents the relatively small peaks of almost the same height, suggesting a spectrum for a mixed layer of GC and DLC [8,9]. With increasing N up to $N > 300$, the bonding structure change from sp^3 to sp^2 would be grown again in the area ablated with $N < \sim 300$. This structural change leads to an increase in the ablation to reverse the crest and trough in the initial interference pattern, while the trough created with $N < \sim 130$ would continuously be swelled due to the bonding change with the pump pulse. We have observed such a reversed interference pattern at $N > \sim 400$. The signal for R is peaked again with a further increase in N , as shown in Fig.3(c). With $N \sim 500$, the deepest nanostructure is formed, where the second peak of R is observed, as seen in Fig.6, as well as the clear change from DLC to GC, as shown in Fig.7(c). Thus, the preferential change in the bonding structure or the morphological structure would rather alternatively be repeated with an increase in N until the original DLC layer is completely removed.

As mentioned above, the present results demonstrate that the thin DLC-film layer stores a part of the incident laser pulse energy through the change in its bonding structure. This bonding structure change increases free electron or electron-hole pair density in the modified area shot by shot. The free electron density would not be uniform on the focal spot of DLC surface to create a local field modulated on a nanometer scale that is much smaller than the laser wavelength. Such a localized field could be strong enough to initiate the nanometer-scale ablation on the surface. In fact, the present experiment have shown that a small field modulation created by the probe pulse can produce a large morphological change or the interference pattern on the surface through the accumulation of incident pulse energy, as shown in Fig.4(b), where the probe pulse fluence used is only 1/700 of the pump. We are making further experimental and theoretical studies to understand the detail of physical processes for the local field generation and resulting nanostructure formation.

5. Conclusions

We have investigated the reflectivity change on the fs-laser irradiated DLC surface, using the pump and probe technique, to understand the interaction processes

responsible for the change from DLC to GC and the nanostructure formation. It has been shown that the initial characteristic enhancement of reflectivity observed is certainly due to the selective change in the bonding structure from sp^3 to sp^2 to induce the swelling of the film surface. From the viewpoint of experiment, this suggests that the pump-probe measurement has successfully resolved the ultrafast evolution between the bonding structure change and the nanostructure formation, while these have been observed under almost the same conditions in the previous experiments [8,9]. The results obtained demonstrate that the nanostructure formation on the DLC surface is certainly preceded by the change in the bonding structure from DLC to GC. Based on the results obtained, we propose that a moderate increase in free electrons coherently produces a local field on a nanometer level, and this local field plays an essential role to form the periodic nanostructure on the film surface.

References

- [1] "Ultrafast Lasers, Technology and Applications" ed. by M.E. Fermann, A. Galvanauskas, and G. Sucha, (Marcel Dekker Inc., New York, 2003).
- [2] S. Nolte, C. Momma, H. Jacobs, A. Tünnermann, B.N. Chichkov, B. Wellegehausen, and H. Welling: J. Opt. Soc. Am. B **14**, (1997) 2716.
- [3] N. Yasumaru, K. Miyazaki, and J. Kiuchi: Appl. Phys. A **76**, (2003) 983.
- [4] N. Yasumaru, K. Miyazaki, J. Kiuchi, and H. Magara: Proc. 5th Int. Symp. on Laser Precision Microfabrication, Nara, (2004) p.755.
- [5] N. Yasumaru, K. Miyazaki, and J. Kiuchi: Appl. Phys. A **81**, (2005) 933.
- [6] Zhou Guosheng, P.M. Fauchet, and A.E. Siegmen: Phys. Rev. B **26**, (1982) 5366.
- [7] J.E. Sipe, Jeff F. Young, J.S. Preston, and H.M. van Driel: Phys. Rev B **27**, (1983) 1141.
- [8] N. Yasumaru, K. Miyazaki, and J. Kiuchi: Appl. Phys. A **79**, (2004) 425.
- [9] K. Miyazaki, N. Maekawa, W. Kobayashi, M. Kaku, N. Yasumaru, and J. Kiuchi: Appl. Phys. A **80**, (2005) 17.
- [10] A. Grill: Diamond Relat. Mater. **8**, (1999) 428.
- [11] G. Dumitru, V. Romano, H.P. Weber, S. Pimenov, T. Kononenko, M. Sentis, J. Hermann, S. Bruneau: Appl. Surf. Sci. **222**, (2004) 226.
- [12] T.V. Kononenko, V.V. Kononenko, S.M. Pimenov, E.V. Zavedeev, V.I. Konov, V. Romano, and G. Dumitru: Diamond Relat. Mater. **14**, (2005) 1368.
- [13] J. Robertson: Pure & Appl. Chem. **66**, (1994) 1789.
- [14] J. Robertson: Advanced In Physics **35**, (1986) 317.
- [15] B.E.A. Saleh and M.C. Teich: "Fundamentals of Photonics", (John Wiley & Sons, Inc., New York, 1991) p.143.

(Received: May 25, 2006, Accepted: May 14, 2007)